Estimating plant stem emerging points (PSEPs) of sugar of beets in early growth stages

Midtiby, Henrik Skov; Mosgaard Giselsson, Thomas; Jørgensen, Rasmus Nyholm

Published in:
Biosystems Engineering

DOI:
10.1016/j.biosystemseng.2011.10.011

Publication date:
2012

Estimating plant stem emerging point of beets in early growth stages

H. S. Midtiby[a,*], T. M. Giselsson[a], R. N. Jørgensen[a]

[a]*Institute of Chemical Engineering, Biotechnology and Environmental Technology, University of Southern Denmark, Niels Bohrs Allé 1, 5230 M, Denmark*

Abstract

Successful intra–row mechanical weed control of sugar beet (*beta vulgaris*) in early growth stages requires precise knowledge about location of crop plants. A computer vision system for locating Plant Stem Emerging Point (PSEP) of sugar beet in early growth stages was developed and tested. The system is based on detection of individual leaves; each leaf location is then described by centre of mass and petiole location. After leaf detection were the true PSEP locations annotated manually and a multivariate normal distribution model of the PSEP relative to the located leaf was built. From testing the system, PSEP estimates based on a single leaf have an average error of $\sim 3mm$. When several leaves are detected the average error decreases to less than $2mm$.

Keywords: plant center, machine vision, leaf extraction

1. Introduction

Mechanical inter-row weeding between crop rows have been used for a long time. But mechanical intra–row weeding within rows between the single crop plants is relatively new. Physical intra-row methods can in general rely on three different strategies (Griepentrog and Dedousis, 2010): (1) soil coverage of weeds or (2) weed root/stem cutting or (3) uprooting of weeds (whole plant or partly). The first option is only relevant in some crop types like cereals and potatos. Sugar beet (*beta vulgaris*) at dicotyledon stage does not belong to these groups(Melander, 2000; Kouwenhoven, 1997) and only strategy two and three may be used.

Several intra–row mechanical weed management methods need to know where the crop plants are located especially with concern to the Plant Stem Emerging Point (PSEP) which is defined as the point where the plant stem emerges from the soil surface. Computer vision was used by (Tillett et al., 2008) to locate transplanted cauliflower plants, before a cultivation disc is moved such that the crop plants are not harmed. RTK–GPS have been used to mark the position

*Corresponding author. E-mail address: hemi@kbm.sdu.dk (H. S. Midtiby)

of crop seeds during sowing (Griepentrog et al., 2005), but the PSEP is not identical to the planted seeds position, as the orientation of the seed have not been taken into account. (Nørremark et al., 2008) used the RTK GPS coordinates to control a cycloid hoe doing intra–row weed control based on seed positions. Uncertainty in seed orientation, PSEP, and GPS accuracy limits the achievable precision to approx $30mm$. (Sun et al., 2010) used RTK–GPS for mapping transplanted tomatoes, 95% of the plants were within $51mm$ from the true plant position. Based on vision input the crop plant positions may be determined with at higher accuracy and precision as (Åstrand and Baerveldt, 2002) indicated by guiding an autonomous weed robot with $20mm$ accuracy along crop rows. Earlier work on extraction of individual leaves from images include (Franz et al., 1991) which analysed boundary curvature by comparing with a known leaf shape and (Neto et al., 2006) which detected individual leaves in complex scenes based on Gustafson–Kessel clustering. This paper describes and evaluates a vision based method which detects single crop leaves and predict where the corresponding PSEP is located.

2. Materials and methods

The current work consists of three parts: (1) development of a leaf detector, (2) building of a relative PSEP model, and (3) using the relative PSEP model to predict true PSEP based on detected leaves. An example image of sugar beet plants in early growth stages is shown in figure 2. The leaves can be described as convex objects with a thin stem (petiole). Leaves are detected by locating convex regions of the plant contour. The relative PSEP model is generated by comparing manually marked PSEP locations (ground truth values) with the detected leaves. Based on the relative PSEP location model and detected leaves, estimates of the true PSEP locations are obtained automatically. Finally are the methods for evaluating performance described.

2.1. Image acquisition and segmentation

Images from sugar beet fields were acquired by a bi-spectral line scanning camera mounted on the Robovator (Poulsen, 2010) intra-row mechanical weeding robot. The setup for image capturing is shown in Fig. 1. The imaged sugar beet plants were part of field emergence trials conducted by Maribo Seed in 2009. Precise plant placement is not required for field emergence trials which can be seen directly in the acquired images where sugar beet plants are distributed randomly over the captured region. The captured area was illuminated with two $55W$ halogen lamps. Each line in the acquired image consists of 256 pixels and a typical data file consist of approximately 13,000 scan lines. A single pixel measured approximately $1.1mm \times 1.1mm$. A sample image can be seen in Fig. 2. For each pixel both a red and a near infrared value are available. Combining red and near infrared values makes it possible to segment images into plant material and soil which is done by calculating the NDVI value for each pixel (Backes and Jacobi, 2006). After this operation a single channel image is obtained with plant material having a high NDVI value compared to soil. This image is segmented using a threshold of 0.2 to form a binary image, the threshold was found by trial and error. These binary images are the basis for the data material used in this paper. Before further analysis are connected components located. It is assumed that a leaf will only contribute to one connected blob. To remove noise only blobs with an area larger than 160 pixels are kept.

2.2. Leaf extraction

For detecting leaves the general leaf structure is exploited. Examples of leaf shapes are shown in Fig. 2. The structure consists of a large mainly convex region attached to the rest of the plant via a thin stem (petiole)(Meier, 2001). The leaf extraction method works in two steps. First convex regions are located and marked as leaf tip candidates, this is described in section 2.3. From the located leaf tip candidates a search for the corresponding petiole is then initiated, the search process is described in section 2.4. If a petiole is located a leaf is found. When a leaf is detected the leaf location and orientation is described by petiole location $\vec{S}$ and the leaf centre of mass $\vec{C}$.

2.3. Leaf tip candidate location

In this section a method for locating leaf tip candidates within the segmented images is described. Leaf tip candidates are found at local curvature minima in curvature of the plant boundary. At this stage is the plant boundary specified as the list of coordinates $\vec{z}_k$ where $k \in [1, \ldots, n]$ and the boundary is followed clock wise. The curvature is then defined as the angle between the line connecting point $k - \Delta$ and k and the line connecting point k and $k + \Delta$. The sign of the direction change indicates whether the current location of the boundary is concave or convex. In this paper the parameter $\Delta = 12$ was used together with a running average of the five nearest points. Plant boundary and curvature along the boundary is visualized in Fig. 3. Local maxima corresponds to concave regions, which are often located at leaf intersections or near the sugar beat growth point, which is assumed to be vertically above PSEP where several leaves are connected to a common area. Local minima corresponds to convex regions such as leaf tips.

To locate a single leaf tip candidate for each leaf, the following steps are used: (1) division of the boundary into concave and convex regions, (2) locate the minima in each convex region and (3) thresholding of the located minima. The purpose of the first step is to split the boundary into segments that at most contain a single leaf tip. As splitting points are used locations where the curvature changes from positive to negative or from negative to positive values. The second step finds the most likely leaf tip location, which are the points along the boundary where the boundary is convex and change of direction is maximized. Step three removes possible leaf tip locations according to direction change, if the direction change is too small (less than 1 radians) the candidate is eliminated.

2.4. Location of corresponding petiole

From each of the candidate leaf tips a search for the corresponding petiole is then initiated. Two walkers are placed at the leaf tip with the goal of following the boundary in each direction, one clockwise and one counter clockwise. The movement of the walkers is controlled such that they will reach the petiole nearly simultaneous. Each walker is then moved forward until the next step along the boundary will bring the euclidean distance between the walker and the leaf tip point above a specified threshold distance l. Then the distance between the walkers is measured. This process (walker movement and distance measurement) is repeated with increasing values of l. In Fig. 4 the search strategy is visualized. For each value of the distance threshold the corresponding circle is drawn together with the two walker locations.

To locate the petiole the distance between the walkers are investigated as follows: (1) search for a narrow leaf region which initiates the region in which the petiole can be located followed by a (2) search for a broadening of the leaf width which ends the region in which the petiole can be found. This strategy was implemented as a state machine. The state machine starts in the leaf–tip state and remains there until the distance between the two walkers get below half of the maximum distance between the walkers and the stage is changed to the leaf–stem stage. While in leaf–stem stage the system keeps track of the minimum distance between the walkers and corresponding walker locations. When the distance between the walkers exceed three times the minimum distance observed in the leaf–stem stage the search is terminated. The leaf boundary cutoff positions are given by the location of the walkers where the distance between the walkers are minimized within the leaf–stage. The petiole location is set to the midpoint of the two boundary cutoff positions. To avoid infinite loops petiole search is terminated if one of the walkers reach a leaf tip candidate or the two walkers pass each other.

2.5. Manual marking of root / leaf relative locations

After the automatic extraction of plant leaves as described in section 2.2, real PSEP location were marked manually. A program showed each plant and the user should then mark the pixel nearest the true PSEP. Fig. 5 illustrate a sample image with PSEPs marked with red spots and detected leaves marked by orange. To describe the marked PSEP location relative to the extracted leaf, the leaf coordinate system is placed with origin located at the petiole $\vec{S}$ and direction of the x axis parallel to the vector $\vec{C} - \vec{S}$. An example is shown in Fig. 6.

The manual annotation of the location of the true PSEP locations is prone to errors. PSEP locations were marked with a single pixel, so the average quantization error will be $\sim 0.5mm$ along each dimension. The true PSEP locations marked by a person will also have an uncertainty. To estimate size of the typical error in this process the same image was annotated by two persons. Differences in PSEP locations were calculated and mean distance between annotations were determined.

2.6. PSEP location model

A multivariate normal distribution is used to model the PSEP location within the leaf coordinate system. The model is defined as:

$$p(\vec{x}) = \frac{1}{2\pi\,|\Sigma_{lc}|}\exp\left[-\frac{1}{2}(\vec{x}-\vec{x}_{lc})^T\Sigma_{lc}^{-1}(\vec{x}-\vec{x}_{lc})\right] \tag{1}$$

where $\vec{x}_{lc}$ is the centre of the true PSEP estimate and Σ_{lc} is the covariance matrix. Both $\vec{x}_{lc}$ and Σ_{lc} are expressed in the leaf coordinate system. Ellipses are used to visualize the multivariate normal distribution, contours of certain values are drawn such that a given fraction of the probability is inside the ellipses. To calculate the ellipses the formula below is used:

$$(\vec{x}-\vec{x}_{lc})^T\Sigma_{lc}^{-1}(\vec{x}-\vec{x}_{lc}) = \chi^2_{2,\alpha} \tag{2}$$

where $\chi^2_{2,\alpha}$ is the χ^2 distribution with 2 degrees of freedom and P value $1-\alpha$. Typical fractions used for visualization are 68%, 95% and 99.7%. As the PSEP is defined relative to the leaf (Fig. 6) the x and y coordinate values translate to a displacement along the major leaf axis and displacement perpendicular to the same axis respectively. The PSEP is expected to lie in extension of the primary leaf axis (low y values) shifted to negative x values. For later analysis position and uncertainty parameters are converted to the global coordinate system using a coordinate transformation based on rotation and translation.

2.7. Combination of relative PSEP location models

In many cases is it possible to detect more than a single leaf, an example is shown in Fig. 7. In the figure 99.7% ellipses of the two estimates of the true PSEP share a common region and it is expected that the true PSEP is located within this region. To combine two PSEP models ($p_A(\vec{x})$ and $p_B(\vec{x})$) the probability densities are multiplied and normalized.

$$p_C(\vec{x}) \propto p_A(\vec{x}) \cdot p_B(\vec{x}) \tag{3}$$

If the PSEP models are defined by the parameters Σ_A, Σ_B, $\vec{x}_c^A$ and $\vec{x}_c^B$ the parameters of the combined model can be expressed as (Gales and Airey, 2006)

$$\Sigma_C^{-1} = \Sigma_A^{-1} + \Sigma_B^{-1} \tag{4}$$

$$\vec{x}_c^C = \Sigma_C\left(\Sigma_A^{-1}\vec{x}_c^A + \Sigma_B^{-1}\vec{x}_c^B\right) \tag{5}$$

This combination of PSEP models is based on the same principle as least squares estimation in the Kalman filter.

2.8. Generation of position predictions

To test the developed method for PSEP estimation, the method was applied to a test image. True plant locations were determined manually and compared to six sets $D_{1,\ldots,6}$ of predicted PSEP locations. These sets were used to measure accuracy of the located PSEPs under different conditions, eg. different number of detected leaves per plant.

From all the detected leaves were a PSEP generated (using only information from this leaf). This is set D_1. D_2 contains PSEPs calculated from two detected leaves. All possible combinations were tested and leaf pairs was combined if distance between centers of their PSEP models was less than $20mm$. D_3 and D_4 are similar to D_2 except that 3 and 4 leaves are used for calculating the PSEP. For a plant where n leaves was detected, the set D_k would contain $\binom{k}{n}$ elements related to that plant. Not all plants had all four leaves detected, therefore will D_4 not contain PSEPs associated to these plants so when the number of leaves used to calculate PSEPs is increased, will the precision of the located PSEPs increase, but a larger fraction will be missed. D_5 is a compromise between large coverage and low placement error. The set is built on D_1 by merging PSEP models with a distance between predicted plant centers of $20mm$ or less. This merging scheme will generate combined PSEP models based on position information from up to 4 leaves. In addition were a set, D_6, generated by manual annotation by a different person than the one who marked the reference PSEPs. D_6 covered only one third of the test image and was used to estimate uncertainty of the manually marked PSEPs.

2.9. Performance evaluation

Performance of the PSEP location model were judged according to the following values:

False positives: If a leaf is falsely found by the leaf separator method it constitute a false positive. These cases are characterized by having a long distance from the predicted PSEP to the nearest true PSEP. False positives are detected by setting a threshold on the allowed distance from predicted leaf location to the nearest true PSEP.

Missed PSEP locations: If none of a plant's leaves have been detected a PSEP is missed. It is characterized by having a long distance from the true PSEP to the nearest predicted PSEP. Missed PSEPs are detected by setting a threshold on the allowed distance.

Predicted position error: The error in the predicted PSEP location were averaged for all predicted PSEP locations with an error less than a threshold of $20mm$.

3. Results

3.1. Leaf detector performance

For evaluating performance of the leaf detector, the 805 leaves present in the test images were counted manually. The leaf detector located 46.6% (395) leaves, of those 2.4% (19) were false positives.

3.2. Relative PSEP model

The leaf detector were applied to three datasets. True PSEPs were marked by hand in all three datasets. Additionally leaves were detected by the leaf detector method and their location specific information recorded. Analyzing leaves and PSEPs led to the generation of 223 data points. In the local leaf coordinate system the multivariate normal distribution model is described by the parameter values:

$$\vec{x}_{lc} = \begin{pmatrix} 5.40 \\ 0.24 \end{pmatrix} mm \qquad\qquad \Sigma_{lc} = \begin{pmatrix} 12.65 & 1.28 \\ 1.28 & 2.35 \end{pmatrix} mm^2 \tag{6}$$

3.3. Fraction of PSEP locations found

The fraction of missed PSEPs is visualized as a function of the chosen threshold in Fig. 8. All six PSEP prediction methods show the same trend. At first the fraction of missed PSEPs decreases linearly until the curve flattens out. The point where the curve flattens out indicates the maximum error of the position estimate and the fraction of PSEPs that are not found. Note that humans are good at locating a large fraction of the PSEPs. The fraction of roots not found within $20mm$ are shown in the MR column in Tab 1. If a single leaf (D_1) is used to predict PSEPs approximately 10% of the true PSEPs will be missed, this number increases strongly when the number of leaves used in the prediction is increased. $\sim 37\%$ of the true PSEPs are missed with estimates based on two leaves, this number is increased to $\sim 89\%$ when four leaves are used to generate estimates. This increase in fraction of missed PSEPs is only to be expected, as the plants with one or two detected leaves are not present in D_3 and D_4.

3.4. Fraction of false positives

To gain insight in the accuracy of PSEP–location–estimates the fraction of false positives is visualized as a function of threshold distance in Fig. 9. The figure is divided into four regions, each representing a dataset. In dataset *One* is the PSEP near which the leaf detector found a single leaf; in *Three* the leaf detector located three leaves. From the green curve it is seen that $\sim 20\%$ of the D_1 position–estimates have a distance (error) of more than $4mm$ to the nearest true PSEP, for comparison is the corresponding distance for D_2 $3mm$. The figure shows that when the number of leaves used to generate a PSEP–location–estimate is increased the error in the estimate is reduced significantly. The figure was divided into four underlying data sets such that each dataset could be weighted appropriately. If all the data was shown in one plot it would be difficult to interpret because each set of location estimates was based on a unique dataset. The number of false positives and missed roots for each of the estimate sets is given in table 1. The listed values are found using a threshold distance of $20mm$. In addition the estimate error (distance from estimate to nearest PSEP) is described using the average value and the 95% quantile (95% of the predicted PSEP had an error of less than...).

4. Discussion

The leaf detector is not able to locate all leaves in the test images. This is due to overlapping leaves, leaves with irregular shapes and to a certain extend limitations in the implemented algorithm. Some typical cases are shown in Fig. 10. The petiole search is fragile and will fail if more than a single leaf tip candidate is found in one leaf. In the used leaf definition (convex area with a thin petiole) overlapping leaves can influence both criteria: the combined leaf area is not guaranteed to be convex and the petiole region can be hidden or widened. Rarely will the relative location of leaf tip estimate and petiole cause the petiole search strategy to fail, this is the case when distance between petiole and leaf tip estimate is less than the distance between leaf tip estimate and the true leaf tip. To reduce the fraction of missed PSEPs the leaf detector must be improved. If a PSEP is not located none of the associated leaves have been detected.

Before evaluation of the implemented algorithms the uncertainty of the true PSEP position should be investigated. This can be achieved by comparing true PSEPs with PSEPs determined by a human being different from the one who determined the true PSEPs initially. The difference between such two manual annotations can be used as an estimate of the position uncertainty of the true PSEPs. On average the difference was $1.37mm$ and in 95% of the cases the difference between the two human annotations were less than $3.58mm$. Two sources contribute to this difference (1) quantification error and (2) uncertainty / unreliability of the human annotation. The quantification error origins from the annotation program, which used integer coordinates for describing PSEPs. A rough estimate of this error is $\pm 0.5mm$ along the two coordinate axes. The human annotation unreliability origins from differences in test image interpretation.

When the leaf detector has found two leaves of a single plant the corresponding true PSEP will with a probability of 95% be within a distance of $5mm$ or less from the guess. This and similar values are shown in table 1. (Sun et al., 2010) positions 95% of the plants within $51mm$. The accuracy of the vision system is thus one order of magnitude better than RTK-GPS seeding of plants. When three or more leaves are used to predict PSEPs the accuracy is comparable to the human annotation. One interpretation of this is that the developed method can predict PSEPs with a higher accuracy than the reference predictions based on manual annotation given that two or more leaves are detected for each PSEP.

5. Conclusion

A system for automated PSEP estimation of sugar beet plants (in growth stages BBCH10-14) based on leaf detection has been developed and tested. In a set of test images the system detected 46.7% of the present leaves. A multivariate Gaussian PSEP model was built based on the detected leaves and manual annotation of true PSEPs. Given centre of mass and attach point of a single leaf the model states that the average true PSEP will be at a distance of $6.2mm$ from the petiole attachment point and placed on the line connecting the leaf attach point and the leaf centre of mass. 95% of the volume below the multivariate Gaussian is contained within an ellipse with semi major and semi minor axes of $12mm$ and $6mm$ respectively.

In the set of test images the detected leaves were used to predict the true PSEPs. With PSEP prediction based on single leaves were 90% of the true PSEPs located within $20mm$ of at least one predicted PSEP location. In this case where the average distance from predicted location to true PSEP of $3.3mm$. When several leaves of the same plant are detected, the PSEP models can be combined using least–squares estimation and thus produce an even better estimate of the true root location. E.g. by combining two leaves the average error is reduced to $1.9mm$. Precise quantification of error in three and four leaf based PSEP estimates is hindered as these methods perform on par with the human annotation used as reference.

Backes, M., Jacobi, J., 2006. Classification of weed patches in quickbird images: Verification by ground truth data. EARSeL European Association of Remote Sensing Laboratories 5 (2), 172–179.
URL http://www.eproceedings.org/static/vol05_2/05_2_backes1.html

Franz, E., Gebhardt, M., Unklesbay, K., 1991. Shape description of completely visible and partially occluded leaves for identifying plants in digital images. Vol. 34. p. 673–681.

Gales, M., Airey, S., Jan. 2006. Product of gaussians for speech recognition. Computer Speech & Language 20 (1), 22–40.
URL http://www.sciencedirect.com/science/article/B6WCW-4FBHW7F-1/2/b1001c29af3057ecce30bf

Griepentrog, H. W., Dedousis, A. P., 2010. Mechanical Weed Control. Vol. 20. Springer Berlin Heidelberg, Ch. 11, pp. 171–179.

Griepentrog, H. W., Nørremark, M., Nielsen, H., Blackmore, B. S., 2005. Seed mapping of sugar beet. Precision Agriculture 6, 157–165, 10.1007/s11119-005-1032-5.
URL http://dx.doi.org/10.1007/s11119-005-1032-5

Kouwenhoven, J. K., 1997. Intra-row mechanical weed control–possibilities and problems. Soil and Tillage Research 41 (1-2), 87 – 104.
URL http://www.sciencedirect.com/science/article/B6TC6-3RGTBJD-7/2/3ce3ed554667f0adfed53e

Meier, U., 2001. Growth stages of mono-and dicotyledonous plants.
URL http://www.bba.de/veroeff/bbch/bbcheng.pdf

Melander, B., 2000. Mechanical weed control in transplanted sugar beet. In: 4th EWRS Workshop on Physical Weed Control.
URL http://orgprints.org/1542/1/Abstract_Elspeet1.pdf

Neto, J. C., Meyer, G. E., Jones, D. D., Apr. 2006. Individual leaf extractions from young canopy images using gustafson-kessel clustering and a genetic algorithm. Computers and Electronics in Agriculture 51 (1-2), 66–85.
URL http://www.sciencedirect.com/science/article/B6T5M-4J2M44F-1/2/b947a39d2c204692a56e44

Nørremark, M., Griepentrog, H., Nielsen, J., Søgaard, H., 2008. The development and assessment of the accuracy of an autonomous gps-based system for intra-row mechanical weed control in row crops. Biosystems Engineering 101 (4), 396 – 410.
URL http://www.sciencedirect.com/science/article/B6WXV-4TX6W5S-1/2/8aede62984cd66ed1ef62a

Poulsen, F., 2010. Measuring emerging plants using machine vision. http://www.visionweeding.com/Products/Plant-Counting/Plant-Counting.htm.
URL http://www.visionweeding.com/Products/Plant-Counting/Plant-Counting.htm

Sun, H., Slaughter, D. C., Ruiz, M. P., Gliever, C., Upadhyaya, S. K., Smith, R. F., Apr. 2010. Rtk gps mapping of transplanted row crops. Computers and Electronics In Agriculture 71 (1), 32–37.

Tillett, N., Hague, T., Grundy, A., Dedousis, A., 2008. Mechanical within-row weed control for transplanted crops using computer vision. Biosystems Engineering 99 (2), 171 – 178.
URL http://www.sciencedirect.com/science/article/B6WXV-4R5H1V8-2/2/4487816230cc4673f885d6

Åstrand, B., Baerveldt, A.-J., Jul. 2002. An agricultural mobile robot with vision-based perception for mechanical weed control. Autonomous Robots 13 (1), 21–35.
URL http://dx.doi.org/10.1023/A:1015674004201

Figure 1: *The camera unit consisted of camera combined with halogen lamp. During image acquisition were eight such units mounted in front of a tractor.*

Set	# leaves	Count	FP	MR	Avg	95%
D_1	1	395	4.8%(19)	10.0%	3.29 ± 0.14	15.76
D_2	2	313	1.6%(5)	37.3%	1.88 ± 0.07	4.62
D_3	3	132	0.8%(1)	70.1%	1.42 ± 0.09	3.02
D_4	4	29	0.0%(0)	89.1%	1.22 ± 0.20	2.39
D_5	1–4	188	8.0%(15)	10.4%	2.66 ± 0.21	49.51
D_6	na	71	0.0%(0)	2.7%	1.37 ± 0.26	3.58

Table 1: *Count: Number of position estimates. FP: False positives, percentage of predicted plant positions with a distance to the nearest true plant location larger than* 20*mm. MR: Missed roots, percentage of true PSEPs within* 20*mm of a predicted PSEP location. Avg: Average estimate error in mm. 95%: 95% quantile of estimate errors in mm.*

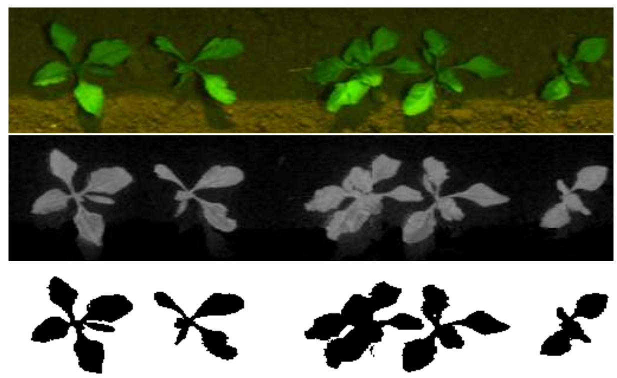

Figure 2: *Plant segmentation was done in two steps. First were NDVI values calculated for each pixel, then was the image thresholded. The shown images are (a) pseudo RGB image of raw data (red is shown as red and NIR is shown as green while the blue channel is set to zero) (b) NDVI image before thresholding and (c) after thresholding.*

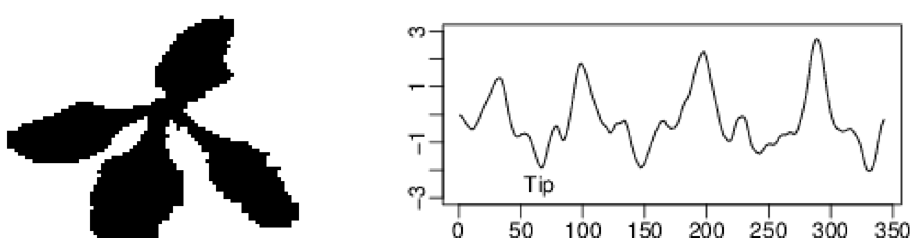

Figure 3: *Example of plant boundary and the calculated curvature along the boundary. The boundary is followed clockwise. Leaf tips are local minima and locations near the PSEP corresponds to peaks.*

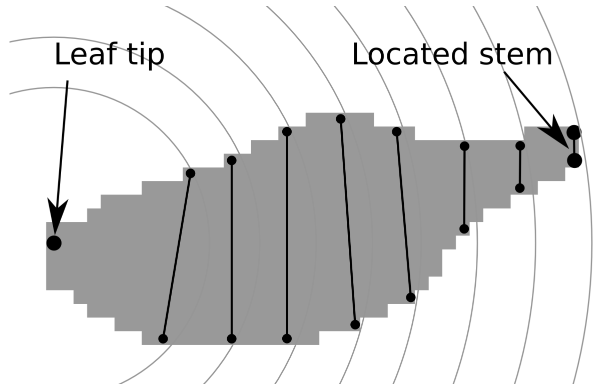

Figure 4: *Visualization of the search strategy. The boundary is followed from the leaf tip until the euclidean distance between the current location and the leaf tip exceeds a specified threshold. This is done in both directions and distance between the located points is measured. The procedure is repeated with increasing distance thresholds illustrated by concentric circles. When distance between located points is minimized the leaf cut–off location is found.*

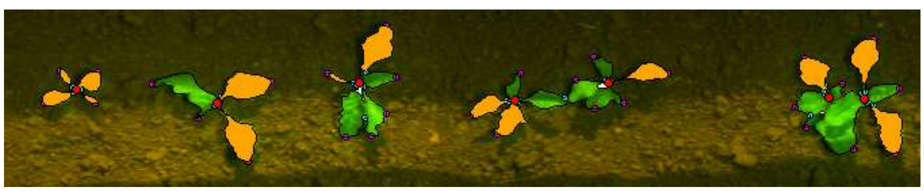

Figure 5: *Manually marking of PSEPs. The orange leaves were detected by the leaf detector. PSEPs are marked with a red spot.*

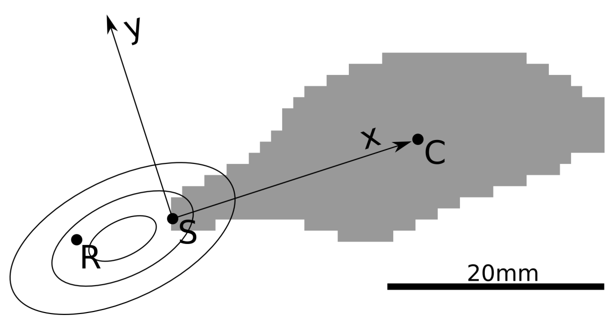

Figure 6: *PSEP location as specified in the leaf coordinate system. The following points are marked: centre of mass C, stem attach point S and PSEP location R. The PSEP location model is indicated by the three concentric ellipses. According to the PSEP location model, will 68% of the true PSEP locations be placed within the central ellipse, the two other ellipses will contain 95% and 99.7% respectively.*

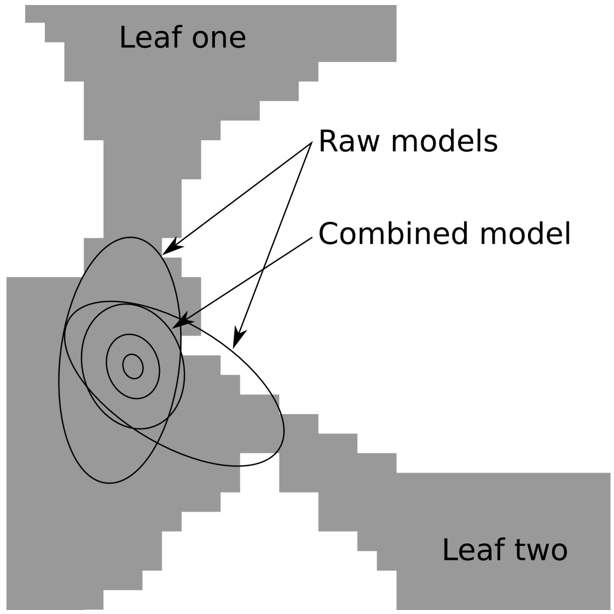

Figure 7: *Combination of two PSEP location models. The ellipses contains are similar to those shown in figure 6. For the raw models are the ellipse for 99.7% shown and for the combined model: 68%, 95% and 99.7%.*

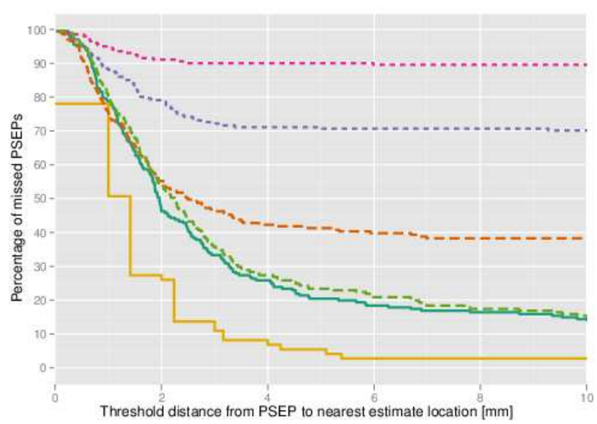

Figure 8: *Fraction of missed PSEPs as a function of the threshold distance. When the number of leaves used to estimate true PSEPs are increased the fraction of missed PSEPs also increases. The following color encoding is used:* ■ *D1,* ■ *D2,* ■ *D3,* ■ *D4,* ■ *D5 and* ■ *D6*

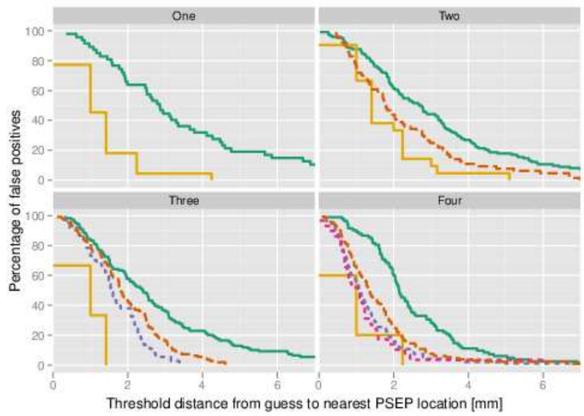

Figure 9: *Fraction of false positives as a function of the threshold distance. Error of PSEP–location–estimates is seen to decrease when the number of leaves used to make the estimate is increased. Color encodings as in figure 8.*

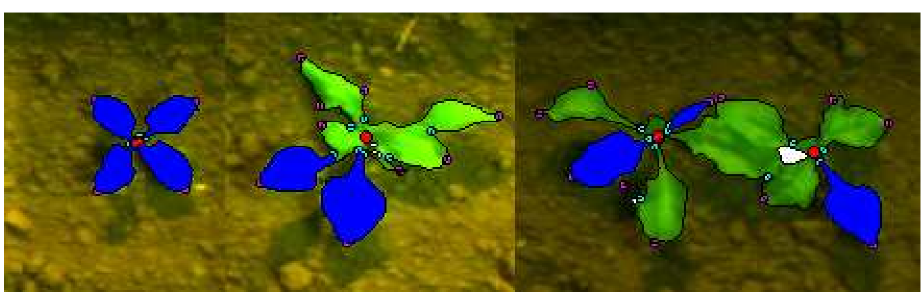

Figure 10: *Easy and difficult cases for the leaf detector. Leaf tip candidates are marked by purple squares. Cyan indicates concave locations. Detected leaves are marked in blue.*